

MONITORING TEMPERATE GLACIER WITH HIGH RESOLUTION AUTOMATED DIGITAL CAMERAS – APPLICATION TO THE ARGENTIÈRE GLACIER

R. Fallourd^{a,b,*}, F. Vernier^a, J.-M. Friedt^c, G. Martin^c, E. Trouvé^a, L. Moreau^d, J.-M. Nicolas^b

^a LISTIC, Université de Savoie, 74944 Annecy-le-Vieux, FRANCE - (renaud.fallourd, flavien.vernier, emmanuel.trouve)^a@univ-savoie.fr

^b LTCI, Telecom ParisTech, 75013 Paris, FRANCE – (renaud.fallourd, jean-marie.nicolas)^b@telecom-paristech.fr

^c Institut FEMTO-ST, Dép^t LPMO, 25044 Besançon, FRANCE – (jean-michel.friedt, gilles.martin)^c@femto-st.fr

^d EDYTEM, CNRS Université de Savoie, F-73376 Le Bourget du Lac, FRANCE - moreauluc^d@club-internet.fr

Commission III, WG III/5

KEY WORDS: digital camera, high resolution, one-view geometry, temperate glacier, glacier-velocity estimation, correlation.

ABSTRACT:

In the context of global warming, the monitoring of temperate glaciers is an important issue for economical and security reasons (water and energy resources, falling ice...) and climate change monitoring. In the glaciologist community this monitoring is based on ground measurements yielding specific information about mass-balance and ice flow. Unfortunately the daily variation measurements of the ice flow are impossible because this information is usually determined with annual temporal distance. However, this traditional monitoring can be now completed with alternative measurement devices which make daily monitoring possible: satellite, GPS, camera... Thanks to high resolution digital cameras installed near the Argentière glacier (massif of Mont Blanc, France), an exceptional set of optical images is available. This article aims to discuss the possibility to use it for daily monitoring, in particular to estimate the glacier-velocity with optimized correlation technique.

1. INTRODUCTION

The Argentière glacier is one of the most monitored temperate glaciers in the world because its melting water is caught by the “Société d’Electricité d’Emosson SA”. The goal is to supply a hydroelectric plant with this melting water. For this purpose a network of galleries has been dug into the glacier bed rock, i.e. under the Argentière glacier. With this exceptional environment, original measurements are possible, like the hydrographic variations (Moreau, 1999) and the basal glacier-velocity which is measured by a unique device based on a wheel, named “cavitometer” (Moreau, 2010; Moreau, 1995). In addition, annual surface measurements like mass-balance and displacement of the Argentière glacier have been realized for more than 30 years by LGGE (Laboratoire de Glaciologie et Géophysique de l’Environnement, Grenoble, France) with “ablation stakes” (Vallon, 1998) located on several parts of the glacier.

However, the traditional “ablation stake” measurements are not sensitive to the daily displacement variations along the year. Furthermore this technique is not possible on the seracs fall and cracked part of temperate glacier because of environmental hazard. To obtain a daily monitoring a solution would be the use of a GPS stations, but like the “ablation stakes”, it is not an appropriate technique in scabrous parts of glacier. Since 2007, high resolution automated digital cameras have been installed around the Mont-Blanc massif. Two of these cameras, located on both sides of the Argentière glacier, provide images focusing on the Lognan serac fall (see Fig.1). This paper highlights the Argentière glacier daily monitoring possibilities with this exceptional set of optical images. This potential has already

been investigated to monitor polar glacier with the same type of camera (Friedt, 2008a; Friedt, 2008b). Some displacement measurements obtained through automated digital camera processing techniques are found in the literature (Maas, 2008; Krimmel, 1986; Harrison, 1986). However, most of these applications are not dedicated to areas comparable to the Argentière glacier, namely temperate alpine glaciers with a study focusing on a serac icefall.

This paper is organized as follows: in section 2, the camera characteristics and the displacement measurement techniques are presented. In section 3, the processing chain is described, and the first glacier-velocity results obtained with two cameras are reported and discussed.

2. CAMERA CHARACTERISTICS AND MEASUREMENT TECHNIQUE

2.1 Camera characteristics

The high resolution automated digital cameras installed near the Argentière glacier are based on customized Leica DLux 3 units. These cameras were selected for their excellent optics, high resolution (10 Mpixels) and off the shelf availability.

Digital electronic control was developed with the purpose of being able to update most capabilities of the automated cameras on the field, since the purpose of these experiments is the long term periodic capture of digital images without moving the setup, and hence keeping the same field of view over time. Hence, most of the development is based on software running on a low-power Texas Instruments MSP430F149

* Corresponding author.

microcontroller. Additional hardware includes an analog switch, power supply management and external low-frequency quartz resonator. With such considerations in mind, a software-defined real time clock runs on the microcontroller and wakes up every second. The interrupt routine compares the current time with the next alarm time at which the camera must be awoken, and runs the camera triggering routine if necessary. Furthermore, the same routine checks whether the user has connected a communication cable and, if so, runs communication software for interacting with a user interface allowing the definition of the current time, camera triggering interval and number of images taken every day.

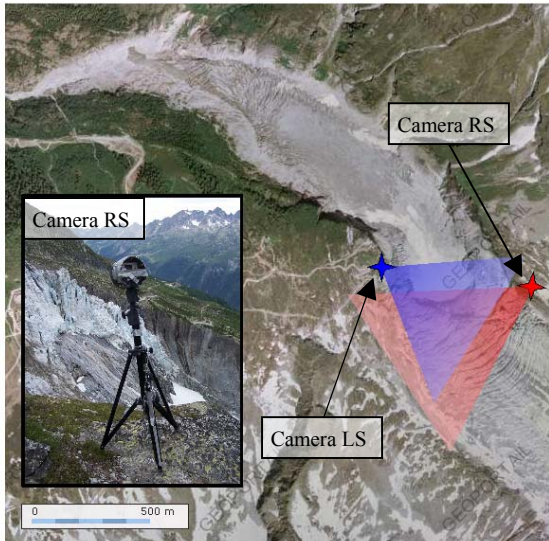


Figure 1. Position of RS (Right Side) and LS (Left Side) cameras focusing to Lognan serac fall of the Argentière glacier (background source: www.geoportail.fr).

The camera is supplied by a 5-V linear voltage regulator with shutdown: hence, when the camera is not running to grab an image, no power is supplied. This strategy was selected since the USB input of the camera exhibits an unacceptable leakage current which would significantly reduce the lifetime of the setup. However, due to this design selection, the last challenging step is the picture time stamping using the internal real time clock. The internal manganese battery is hardly accessible, and exhibits a life-expectancy of a few months. Since time stamping is mandatory for quantitative motion analysis, we have added external solar panels to supply power to the camera in order to refill the internal real time clock battery.

Camera characteristics	
Number of pixels	10 M
Image size (columns × lines)	4224 × 2376
Aperture angle (α_a)	2.7×10^{-4} rad./px.

Table 1. Characteristics of RS and LS cameras.

Hence, the only connexion between the power management circuit and the camera is through a 4066-analog switch. The camera stores its images on a SD card, accessible to the user without breaking the seal keeping the camera dry. The angle of view of the camera was calibrated and observed to be 65 degrees. The 10 Mpixel mode generates pictures 4224 pixel wide so that the angle of view of a single pixel is 0.015 degrees (aperture angle).

2.2 Displacement measurement technique

In the field of image processing, the correlation technique is commonly used to correct image motion (Zitová, 2003). This method is also commonly used to estimate a displacement within a set of optical images (Berthier, 2005; Maas, 2008). It is also used in stereovision to compute Digital Elevation Models (DEM) (Toutin, 2002) or to provide glacier 3D models (Rivera, 2008; Pitkänen, 2003 ; Brecher, 1993).

The principle of the “correlation” technique consists in using the intercorrelation function as a criterion to measure the similarity between sub-images, and to search for the position of the maximum to derive the relative displacement. Different similarity functions can be used: centred correlation (subtraction of the local means), normalised correlation (as used hereafter, see Eq. 2), or normalized centred correlation (covariance divided by the product of the standard deviations). The computation of these “correlation” criteria can be performed either in the temporal (spatial) domain or in the frequency domain by using a 2D FFT (Fast Fourier Transform) to reduce the number of operations from N^2 to $N \log(N)$ where N is the number of samples of the subwindows. This approach is used in several software dedicated to displacement measurement in remote sensing: COSI-Corr (Ayoub, 2009), IMCORR (<http://nsidc.org/data/velmap/imcorr.html>) or ROI_PAC (http://www.roipac.org/Offset_Tracking) with SAR images for exemple. However, when the correlation is computed for each pixel of the image (for dense displacement fields), optimization techniques based on sliding windows can also strongly reduce the computation load and are more flexible regarding the subwindow size which can be different form powers of 2. In both case, the resulting displacements are quantified by the pixel spacing (except when the phase slope of the FFT products is analysed). To increase the precision, different techniques are possible: oversampling by interpolation in the space domain, or by zero padding in the Fourier domain, or fitting the correlation discrete values by an analytical function.

In practice, we look for a displacement field between two images: the master image $I_m(i,j)$ and the slave image $I_s(i,j)$ after an initial registration on the motion-free parts of the images. For a pixel (i,j) in the master image, the displacement vector $\vec{V}(i,j)$ is obtained by computing the values of a similarity function $sim(p,q)$ between a master block Ω_m centred in pixel (i,j) and the same block Ω_s translated by (p,q) in the slave image. According to a-priori displacement information, the search is made for $(p,q) \in \Delta = [p_{min}, p_{max}] \times [q_{min}, q_{max}]$. The displacement vector estimated in pixel (i,j) is:

$$\vec{V}^d(i,j) = (p_{opt}, q_{opt}) = \underset{(p,q) \in \Delta}{Arg \max} sim(p,q) \quad (1)$$

where (p_{opt}, q_{opt}) is the offset which maximize the similarity function $sim(p,q)$. The resulting displacement measurement based on this optimal position is discreet: (p_{opt}, q_{opt}) are integer numbers and the displacement values are multiples of the pixel spacing. To improve the precision, a sub-pixel measurement $V^{sub}(i,j)$ is computed in two steps. First, the similarity function $sim(p,q)$ is approximated by a second order polynomial function near the position (p_{opt}, q_{opt}) over the 3×3 block $[p_{opt}-1, p_{opt}+1] \times [q_{opt}-1, q_{opt}+1]$. Secondly, the sub-pixel position of the $sim(p,q)$ function maximum is obtained by cancelling the first derivative of the interpolated function in two directions of the image. Finally, using the pixel spacing and the temporal interval Δt between master and slave images, the magnitude and

the orientation of the displacement vector are calculated in m/day and degrees respectively.

The similarity function $sim(p,q)$ used in this article is the normalized correlation (NC). This function is defined as:

$$NC(p, q) = \frac{\sum_{(k,l) \in \Omega_m} I_m(k,l) I_s(k+p, l+q)}{\sqrt{\sum_{(k,l) \in \Omega_m} |I_m(k,l)|^2 \sum_{(k,l) \in \Omega_m} |I_s(k+p, l+q)|^2}} \quad (2)$$

Its maximization corresponds to the minimization of the squared difference between Ω_m and Ω_s sub-images. The NC function was selected rather than the NCC function as it was thoroughly optimized.

This displacement measurement technique has been implemented in C language. This software named `dist_corr` is implemented according to both optimization studies. The former is a mathematical study; it rewrites Eq. (2) such that any operation is computed only once. The later is an implementation study that minimizes the use of “indirections”. The gain of those optimizations is close to three times compared to a “naive” implementation. Another advantage of `dist_corr` software is that it includes multiple processing blocs. In other words it can be split on different cores or machines. Thus, with this approach, the gain is given by the number of cores: the time to compute is divided by the number of cores. The `dist_corr` program is part of EFIDIRtools software. This software, including multiple processing blocs, has been developed by the EFIDIR project (Extraction and Fusion of Information for ground Displacement measurements with Radar Imagery).

3. ESTIMATION OF GLACIER VELOCITY

3.1 Processing chain description

The initial jpeg images (Red-Green-Blue colour format) are converted in greyscale images according to Craig’s formula ($0.3 \times \text{Red} + 0.59 \times \text{Green} + 0.11 \times \text{Blue}$). Next, a co-registration between the images is made on the motion-free parts of the images. Indeed, between the image acquisitions the camera slightly moves because of the weather conditions (wind, temperature...). In practice, the mountain crest lines on the background are used to perform it. This initial image co-registration on motion-free areas is realized by a translation without applying sub-pixel offsets. The advantage is to avoid the resampling of the slave image with a blurring effect due to the interpolation. The disadvantage is that it introduces up to 0.5 pixel error in the displacement estimation. This error is corrected by estimating the remaining offset by the sub pixel NC displacement estimation over fixed areas. Nevertheless this correction is not effective because the geometric deformations caused by the little move of camera are proportional to the scene distance. Finally, the velocity estimation, magnitude and orientation of the displacement vector, is computed with image pairs, i.e. master and slave images. The computation window size is $\Omega_m=31 \times 31$ and $\Delta=21 \times 21$ for the RS camera, and $\Omega_m=31 \times 31$ and $\Delta=25 \times 25$ for the LS camera. The velocity-estimation maps are expressed in pixel/day because the distance between the camera and the scene is not known. The displacement vectors are expressed in the two-dimension (2D) camera geometry. The one-view geometry of the framework provides only the projections of the true 3D displacements in

the image plane (line and column directions). All maps results are presented with a grey mask preserving the areas where the displacements are higher than two pixels because the remaining offsets on fixed area, caused by pixelic co-registration, range from 0 pixel to 2 pixels.

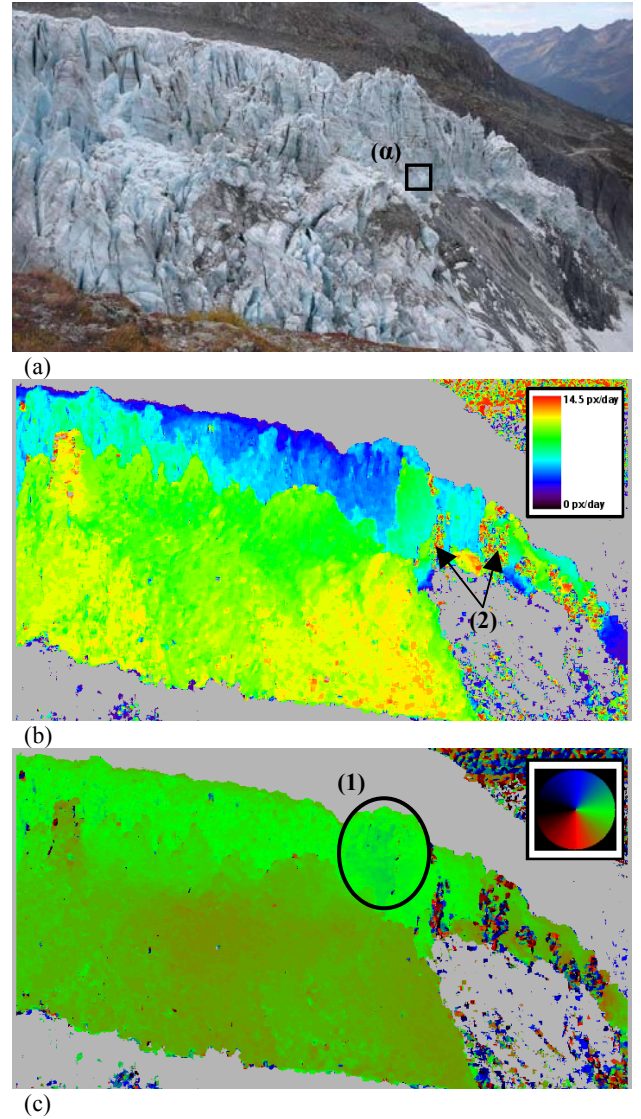


Figure 2. Velocity map estimation of the Argentière glacier computed with RS camera (2008-10-09/2008-10-10 pair). RGB jpeg image (a), magnitude of velocity vector (b) and orientation of velocity vector (c).

To complete the study, the 2D-velocity estimation is expressed in cm/day for blocks (a) (Fig. 2-(a)) and (b) (Fig. 2-(b)) having a size of 100×100 pixels, localized on the basal part of the Argentière glacier. These 2D-velocities expressed in cm/day correspond to the average of velocity vector magnitude and orientation on considered blocks. The computation is realized with three images for both cameras with one day temporal distance Δt . Therefore, for each camera, three velocity estimations are computed, two for $\Delta t = 1 \text{ day}$ and one for $\Delta t = 2 \text{ days}$. The conversion of px/day into cm/day is obtained according to the following expression:

$$\Delta px = d \times \alpha_a \times 10^{-4}. \quad (3)$$

where d is the spatial distance camera-object in meter and α_a is the aperture angle in radian/pixel.

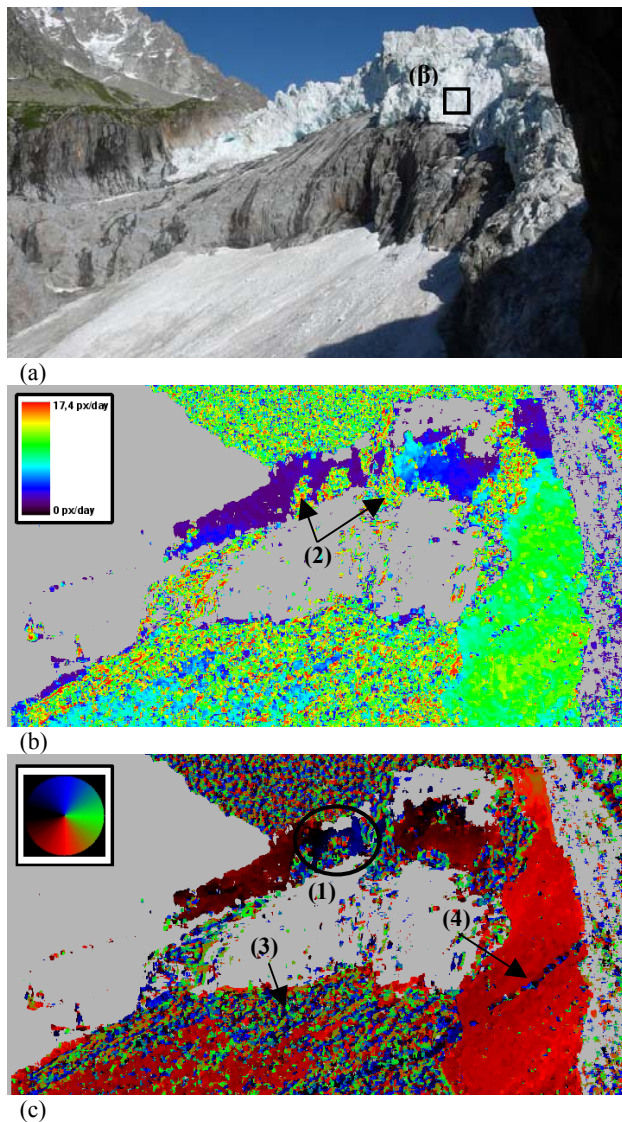


Figure 3. Velocity map estimation of Argentière glacier computed with LS camera (2007-07-14/2007-07-15). RGB jpeg image (a), magnitude of velocity vector (b) and orientation of velocity vector (c).

3.2 First results

The local velocity-estimation map of the Argentière glacier computed with RS and LS cameras are shown in Fig.2 and Fig.3 respectively. For each camera, samples of 2D-velocity expressed in cm/day are presented in Tab.2.

The RS and LS cameras results show that the magnitude map of velocity vectors (Fig. 2-(b) and Fig 3-(b)) is not homogenous according to the different image planes. In the glaciology domain it is known that glacier-velocity is not homogenous. The traditional measurements (“ablation stakes”) proved that the velocity in the center of the glacier is the highest velocity, with a gradient towards the boundary. In this particular case, the magnitude map heterogeneity is not due to the glacier flow physic but to the 2D-velocity expressed in pixel/day. Hence, the nearest parts of the glacier appear to be flowing faster than the farthest parts.

The orientation information is more reliable than magnitude because it is independent of the 2D-velocity expressed

behaviour -pixel/day or cm/day-, i.e. the physical distance between the camera and the scene. Globally the orientation estimation (Fig. 2-(c) and Fig 3-(c)) seems correct. The displacement follows the slope, in particular for RS camera. The estimation shows that the ice follows the breaking slope. The comparison between the two view angles reveals that the glacier rises up in a specific area (see area (1) on Fig. 2-(c) and Fig. 3-(c)). Historically this phenomenon has been observed by glaciologists who currently work on the Argentière glacier. In practice this rise up is due to the glacier bed rock topography.

Several parts of the magnitude and orientation maps show that the glacier-velocity estimation is corrupted by noise. These parts correspond to ice falls (serac) which happen between the two image acquisitions (see mark (2) on Fig. 1-(b) and Fig. 2-(b) to localize them). Therefore the surface is changed and the estimation is wrong (the correlation level is low). In addition, the low part of Argentière glacier, visible in LS camera images, encloses noise. This noise is due to the crushed of the serac falls (see mark (3) on Fig. 3-(c)). The transversal line observed in the orientation map (see mark (4) in Fig. 3-(c)) corresponds to the detection of the shadow.

The 2D-velocity estimation of the Argentière glacier (see Tab.2) shows for both cameras that the values of magnitude and orientation are almost constant for the three pairs. The standard deviation, i.e. error information, gives a good confidence in relation to estimated magnitude and orientation. This confidence is confirmed by the specific relation between the one-day and two-day pairs. Indeed, the sum of displacement of the two one-day pairs is almost equal to the displacement of the two-day pair. Regarding to the one-year temporal distance between the camera acquisition and the two different image planes, the comparison is not exhaustive, but reveals that magnitude estimations are in the same range. Also, glaciology studies have shown that near the serac fall, the glacier basal velocity is 35 cm/day in summer and 20-25 cm/day in winter.

	Images pair	Δt	Magnitude	Orientation
Camera RS (α)	2008-10-16 / 2008-10-17	1 day	44.1 cm/day (3.4)	187.5° (3.8)
	2008-10-17 / 2008-10-18	1 day	45.9 cm/day (3.2)	186.9° (3.2)
	2008-10-16 / 2008-10-18	2 days	45.0 cm/day (3.1)	187.4° (2.9)
Camera LS (β)	2007-07-14 / 2007-07-15	1 day	39.5 cm/day (3.4)	37.4° (5.0)
	2007-07-15 / 2007-07-16	1 day	40.0 cm/day (2.6)	35.6° (3.7)
	2007-07-14 / 2007-07-16	2 days	39.8 cm/day (3.3)	37.7° (4.6)

Table 2. Average velocity estimation computed with blocks (α) (Fig. 2-(a)) and (β) (Fig. 2-(b)) for three images pairs. The standard deviation is given in italic between brackets.

4. CONCLUSION AND PERSPECTIVES

4.1 Conclusion

The high resolution digital camera data set acquired on the Argentière glacier has been processed to evaluate the temperate

glacier monitoring potential. For this purpose, the study has been lead on a specific part of the glacier which has been viewed by two cameras with two different viewing angles. The originality of this work is to estimate glacier-velocity in the most scabrous part of the glacier (Lognan seracs fall) where the traditional measurement techniques like “ablation stakes” are not possible.

In order to estimate the glacier-velocity map, an optimized “correlation technique” is used with one pair of images for each camera. For two specific points, velocity estimation has been computed in cm/day with three pairs for each camera. Regarding to this first study, the Argentière glacier monitoring with high resolution digital cameras is promising. However, the estimated displacement vectors are not expressed in three-dimensions; they are only expressed in the two-dimension camera geometry. Furthermore, the global velocity field is only expressed in pixel/day because the distance between the camera and the scene is not known.

4.2 Perspectives

Daily and seasonal velocity variation estimates should be searched by extending the displacement analysis to a wider sequence of images (several month long series).

Some further work is necessary to improve the processing chain. Firstly, the imaging scene distance will be checked against a Digital Elevation Model (DEM). This step will make global velocity calibration possible. Next, the image registration will be realized according to the imaging scene distance. Nevertheless the most recent DEM available in the Mont Blanc area is from 2004. Since that time, the glacier surface topography has changed.

There are two alternative solutions. The first solution is to install another camera providing a correct stereo vision configuration. This would make the 3D reconstruction and the 3D displacement estimation possible. The second solution is more original: the 3D displacement can be derived by combining a ground based digital camera and high resolution spaceborne SAR data which can be obtained more regularly than spaceborne optical data. TerraSAR-X satellite provides for instance 11-day repeat pass images with up to 1 meter resolution. The first results of assessing the potential of such images to monitor Argentière glacier have been presented in (Fallourd, 2009).

ACKNOWLEDGEMENTS

The authors wish to thank the “Société d’Electricité d’Emosson SA” and the EFIDIR project (ANR-2007-MCDC0-04, <http://www.efidir.fr>) for supporting this work. The automated digital cameras were developed as part of the French National Research Agency (ANR) program Hydro-Sensor-FLOWS under the direction of M. Griselin (Thema, Besancon, France) and C. Marlin (IDES, Orsay, France).

REFERENCES

Ayoub, F., Leprince, S, Keene, L, 2009. User’s guide to COSI-Corr, Co-registration of Optically Sensed Images and Correlation, California Institute of technology, USA. http://www.tectonics.caltech.edu/slip_history/spot_coseis/pdf_files/cosi-corr_guide.pdf (accessed May 2010)

Berthier, E., Vadon, H, Baratou, D., Arnaud, Y., Vincent, C., Feigle, K.-L., Remy, F., Legrésy, B., 2005. Mountain glacier surface motion derived from satellite optical imagery. *Remote Sensing Environ.*, 95 (1), pp 14-28.

Brecher, H., Thompson, L. G., 1993. Measurement of the retreat of the Qori Kalis Glacier in the tropical Andes of Peru by terrestrial photogrammetry. *Photogrammetric Engineering and Remote Sensing*, 59(6), pp 1017-1022.

Fallourd, R., Harant, O., Trouvé, E., Nicolas, J.-M., Tupin, F., Gay, M., Vasile, G., Bombrun, L., Walpersdorf, A., Serafini, J., Cotte, N., Vernier, F., Moreau, L., and Bolon, P., 2009. Monitoring temperate glacier: combined use of TerraSAR-X images and continuous GPS measurements. In: *International Workshop on the Analysis of Multi-temporal Remote Sensing Images (MULTITEMP’2009)*, Groton, USA.

Friedt, J.-M., Ferrandez, C., Martin, G., Moreau, L., Griselin, M., Bernard, E., Laffly, D., Marlin, C., 2008a. Automated high resolution image acquisition in polar regions. In: *12th Alpine Glaciological Meeting*, Chamonix, France.

Friedt, J.-M., Ferrandez, C., Martin, G., Moreau, L., Griselin, M., Bernard, E., Laffly, D., Marlin, C., 2008b. Automated high resolution image acquisition in polar regions. In: *European Geosciences Union*, Vienna, Austria.

Harrison, W.-D., Raymond, C.-F., Mackereth, P., 1986. Short period motion events on variegated glacier as observed by automatic photography and seismic methods. *Annals of Glaciology*, 8, pp 82-89.

Krimmel, R.-M., Rasmussen, L.-A., 1986. Using sequential photography to estimate ice velocity at the terminus of Columbia glacier, Alaska. *Annals of Glaciology*, 8, pp 117-123.

Maas, H.-G., Schwalbe, E., Dietrich, R., Bäessler, M., Ewert, H., 2008. Determination of spatio-temporal velocity fields on glaciers in West-Greenland by terrestrial image sequence analysis. In: *IAPRS*, Beijing,China, XXXVII, Part B8, pp. 1419-1424.

Moreau, L., Polti, A., Danger, J.-L., Nicolas, J.-M., Fallourd, R., and Trouvé, E., 2010. De la roue au radar quelques innovations en métrologie radar. In: *5ème Colloque Interdisciplinaire en Instrumentation (C2I)*, Le Mans, France.

Moreau, L., 1999. Synthèse des variations de l’hydrographie sous-glaciaire du glacier d’Argentière de 1970 à 1999. *La Houille blanche (Revue générale de l’électricité)*, 5(54), pp 40-46.

Moreau, L., 1995. Comportement d’un glacier tempéré sur son lit rocheux. *Phd Thesis, Joseph Fourier university*, Grenoble, France.

Pitkänen, T., Kajutti, K., 2004. Close-range photogrammetry as a tool in glacier change detection. In: *IAPRS*, Istanbul,Turkey, XXXV, Part B7, pp. 769-773.

Rivera, A., Corripio, Javier G., Brock, B., Clavero, J., Wendt, J., 2008. Monitoring ice-capped active Volcán Villarrica, southern Chile, using terrestrial photography combined with automatic weather stations and global positioning systems. *Journal of Glaciology*, 54(188), pp 920-930.

Toutin, T., 2002. Three-dimensional topographic mapping with ASTER stereo data in rugged topography. *IEEE Transactions on Geoscience and Remote Sensing*, 40(10), pp 2241-2247.

Vallon, M., Vincent, C., and Reynaud, L., 1998. Altitudinal gradient of mass balance sensitivity to climatic change from 18 years of observations on Argentière glacier. *Journal of Glaciology*, 146(44), pp.93-96.

Zitová, B., Flusser, J., 2003. Image registration methods: a survey. *Image and Vision Computing*, 21, pp 977-1000.